Preprints (www.preprints.org) | NOT PEER-REVIEWED | Posted: 10 November 2019

Title page

Medicinal Herbal Combination, Chen-Ma-Dan-Sam-Ga-Mi-Bang, Attenuates Hippocampus Neuronal Cell Damage on Hypoxia of Balb/c mice model

Chang-Young Kim[1], Na-Ra Shin[2], Hyuk-Hee Kwon[2], Zhigang Fang[3,4], Dong-Woon Kim[2], Hye-Won Lee [5], In-Chan Seol[6], Yoon-Sik Kim[6], Hyun-Kyoung Cho[6], Hyeong-Geug Kim [1,4,#], and Ho-Ryong Yoo[1,6,#]

[1]*Department of Neurologic Disorders & Aging Brain Constitution, Dunsan Oriental Hospital of Daejeon University, 176, Seo-gu, Daejeon, 35253, South Korea*

[2]*Department of Anatomy, Brain Research Institute, Chungnam National University School of Medicine, Daejeon, Republic of Korea*

[3]*Guangzhou University of Chinese Medicine, Guangzhou 510405, PR China*

[4]*Department of Biochemistry and Molecular Biology, Indiana University School of Medicine, Indianapolis, IN 46202*

[5]*TKM-Based Herbal Drug Research Group, Korea Institute of Oriental Medicine, 461-24, Jeonmin-dong, Yuseong-gu, Daejeon, South Korea*

[6]*Department of Cardiology and Neurology of Korean Medicine, College of Korean Medicine, DaeJeon University*

© 2019 by the author(s). Distributed under a Creative Commons CC BY license.

Preprints (www.preprints.org) | NOT PEER-REVIEWED | Posted: 10 November 2019

Abstract

Incident rates of neurodegenerative diseases have steadily increased globally, but there is no therapeutic access available. We newly prescribed medicinal herbal remedy including five different herbal plants called, *Chen-Ma-Dan-Sam-Ga-Mi-Bang* (CMST), purposed to prove for pharmacological properties and corresponded actions on hippocampus neuronal cell injury by hypoxia-induced mice model. Mice were adapted to normoxia or hypoxia with or without CMST for 5 days. We gathered pharmacological effects of CMST on cell injury by enhancement of dihydroethidium and 4-hydroxynonenal signals which were correlated with abnormal redox status in the protein or gene expression levels (abnormal elevations of nitric oxide, reactive oxygen species, lipid peroxidation and deteriorations of total glutathione, total antioxidant capacity, and activities of superoxide dismutase and catalase) due to hypoxia. CMST also notably exerted to attenuates molecules for neuronal cell injury markers such as p-tau, cleaved caspase-3 due to DNA oxidations (53bp1and phosphor-histone H2AX), inflammatory cytokines, and hemeoxigenase-1. We further figured out the underlying actions of CMST by *in vitro* experiment through inactivation of microglial cell which can mediate neuronal cell injury. Collectively, CMST prevented from hippocampal neuronal cells via inactivation of microglial cell with normalization of redox status on hypoxia-induced hippocampus neuronal cell injury.

Key words: Traditional Korean Medicine, Hippocampus, Neuronal Cell death, Oxidative stress, Medicinal herbs

Preprints (www.preprints.org) | NOT PEER-REVIEWED | Posted: 10 November 2019

Introduction

Brain tissue is one of the most important organs that plays major roles for learning, controlling locomotive functions, modulating of homeostasis for physiological condition through whole body and psycho-emotional status, and physical stress response [1-6]. Physiologically, the brain tissue is elaborately evolved for defensing against pathological conditions, especially brain cell damages condition by neurodegenerative disease [7, 8]. Once brain tissue was damaged, various cell types are complicatedly associated with response to specific cell types to accelerate tissue damages [9-11].

The brain tissue is well known for the most susceptible bio-organism tissue to damage by oxidative stress owing to highly oxygen consumption rate, plenty of iron and peroxidation of fatty acids, and equipped as lower concentration of endogenous antioxidants [12-14]. Continuous oxidative stress condition is deeply associated with inflammatory reactions by enhancement of pro-inflammatory cytokine secretions, including tumor necrosis factor (TNF)-a, interleukin (IL)-6, and IL-1β, and deteriorations of IL-10, mainly from unexpected microglial cells activation [15, 16]. These pathological alterations are mainly characterized by the neurodegenerative diseases including Alzheimer's disease, Parkinson's diseases, Huntington's diseases, and stroke, respectively [17]. Although the morbidity of neuronal degenerative diseases has steadily increased every year in worldwide [18], the exact pathophysiological mechanisms still remain unclearly and no therapeutic access available.

On the other hand, according to traditional Korean medicine (TKM), the above pathological status is mainly provoked by unbalance between *blood* and *qi* streams. Therefore, some of specific medicinal herbs or their combinations have been candidate to treat neurodegenerative diseases underlying pharmacological mechanisms.

Preprints (www.preprints.org) | NOT PEER-REVIEWED | Posted: 10 November 2019

In the clinical practice of TKM, numerous medicinal herbs have been generally treated or administrated to the patients with neurodegenerative diseases. Based on emerging experience of prescribing herbal medicines, we finally selected five pivotal medicinal herbal combinations to treat various neurogenerative dieses especially with neuronal cell damages.

Therefore, we purposed to investigate the pharmacological effects of a medicinal herbal mixture, *Chen-Ma-Dan-Sam-Ga-Mi-Bang* (CMST), which is composed of five herbal plants including *Gastrodia elata* Blume, *Codonopsis lanceolata* (Siebold & Zucc.) Benth. & Hook.f. ex Trautv., *Angelica gigas* Nakai, *Curcuma longa* L. (Zingiberaceae), and *Astragalus mongholicus* Bunge and its underlying actions against neurodegenerative of pre-clinical model specifically adaption of hypoxia-induced neuronal cell damages.

Preprints (www.preprints.org) | NOT PEER-REVIEWED | Posted: 10 November 2019

2. Material and methods

2.1. Chemicals

The dulbecco's Modified Eagle's Medium (DMEM : Gibco BRL, U.S.A.), fetal bovine serum (FBS : Gibco BRL, U.S.A.), penicillin-streptomycin (Sigma, U.S.A.), antibiotic-antimycotic (Sigma, U.S.A.), lipopolysaccharide (LPS : Sigma, U.S.A.), nitric oxide detection kit (Intron Biotechnology, Korea), and dulbecco's phosphate buffered saline (DPBS : Welgene, Korea).

2.2. Preparations of CMST and chemical composition analysis

The CMST, which is a new persribed herbal mixture with water extract, is composed of same amount of five different herbal plants including *G. elata* Blume, *C. lanceolata* (Siebold & Zucc.) Benth. & Hook.f. ex Trautv., *A. gigas* Nakai, *Curcuma longa* L. (Zingiberaceae), and *A.* mongholicus Bunge, respectively. All herbal plants were obtained from the Dunsan Oriental Hospital of Daejeon University under the inspection of the Herbology professor (Daejeon, South Korea). The herbal mixtures (total weights were 500 g) were boiled with distilled water (DW) at 100°C for 4 hrs and filtered with 300 mesh filter (50 μm). Condensing during 1hr of extraction, sample was placed under -70°C for at least 3 hrs for the frozen extract processing. The frozen lyophilization was performed over than 72 hrs and sample was collected and weighed. The final yield was 7.82 % (w/w).

To identify the chemical features and reproducibility of the CMST, fingerprinting analysis was performed using high-performance liquid chromatography-diode array detector-mass spectrometry (HPLC-DAD-MS) for either CMST or its reference compounds; especially for *G. elata* Blume for gastrodin, *A. gigas* Nakai for nodakenin and decursin, and *A. mongholicus* Bunge

Preprints (www.preprints.org) | NOT PEER-REVIEWED | Posted: 10 November 2019

for formonetin, respectively. Briefly, after the dissolution (20 mg of CMST and 0.01 mg of 2 standards in 1 mL 50% methanol) with filtration, and then these formulations were subjected to HPLC analysis of Agilent 1100 series (Agilent Technologies, Santa Clara, CA). The HPLC system consisted of a SCL-10A system controller, LC-10AD pump, SPD-10MVP diode array detector, and CTO-10AS column temperature controller (Shimadzu, Kyoto, Japan). A Phenomenex Prodigy C18 (4.6 × 250 mm; particle size 5 μm; Phenomenex, Torrance, CA) column was eluted with solvents A (10% acetonitrile in water containing 0.1% formic acid) and B (DW) at a flow rate of 0.4 mL/min. Solutions of 15% A and 85% B were changed to 60% B for 30 min, 40% B for 40 min, and 0% B for 60 min. The histograms and quantification analysis were obtained under the condition of 280 and 330 nm (Fig. 1).

2.3. Animal experiment

A total 46 heads of male Balb/C mice (16 weeks old, 26 to 28g) were purchased from Daehan Biolilnk (Choong-buk, South Korea). Mice were housed 6 to 8 per each cage with serving of standard chow diet with distilled water *ad libitum*, and kept under a 12 h light/dark cycle (lights on from 07:30 am to 07:30 pm) under the a constant temperature (23 ± 1°C) and relative humidity (55 ± 5%). After 7 days of adaption period, mice were randomly divided into 6 groups including normoxia (n = 6), hypoxia, CMST 25, CMST 50, CMST 100, and Vit C 100 (n = 8 for each) groups, respectively. Mice were transferred into a gas chamber flushed with one of the following mixtures (balance N_2): 11% ± 1 O_2 for hypoxia condition or 21% ± 1 O_2 for normoxia condition during 4 hours for 5 days after drug administrations. Mice were housed in (40 cm length × 40 cm width × 30 cm height) transparent acrylic boxes. This hypoxia chamber (IEC266-Life, version 1.3) was manufactured in Vision Science. The total gas flow through the chamber was measured using

Preprints (www.preprints.org) | NOT PEER-REVIEWED | Posted: 10 November 2019

a portable LCD touch controller with an O_2 sensor adjusted to O_2 concentrations 11% (programming setting 11% ± 1). Temperature was maintained at 23 to 26 °C, and humidity was maintained at 30 to 70%. Mice were housed in cages in hypoxia chamber with standard bedding and given unlimited access to food and water.

Animal treatment and maintenance were conducted in accordance with the Animal Care and Use Guidelines issued by Chungnam National University. All experimental protocols were approved by the Institutional Animal Care and Use Committee of Chungnam National University (CNU-00955).

2. 4. Cell cultures, generations of hypoxia, and drug treatments

The HT-22 cells (mouse hippocampal neuronal cell line) and BV-2 cells (mouse microglial cell line) were provided from the Department of anatomy from Medical Schoool of Chung-Nam-National University (Especially, served by professor Dong-Woon Kim, Daejeon, South Korea). The cells were cultured in DMEM with 10% FBS and antibiotics (100 U/mL penicillin G and 100 μg/mL streptomycin). The cells were maintained under humidified conditions at 37°C in 5% CO_2. The hypoxia condition in the cell line was cultured in hypoxic conditions (O_2 1%) in a 37°C CO_2 incubator (Thermo Fisher Scientific, Waltham, MA, USA) to perform experiments. The hypoxic condition was generated with BD GasPak™ EZ Anaerobe Gas Generating Pouch System (Becton, Dickinson and Company, Franklin Lakes, NJ, USA).

To investigate protective effects of CMST against hypoxic-induced hippocampus neuronal cell damage, we pre-treated CMST (0 to 100 μg/mL) and transferred to normoxia or hypoxia condition

Preprints (www.preprints.org) | NOT PEER-REVIEWED | Posted: 10 November 2019

for 24 hrs. For verifying microglial cells activation affect to hippocampus neuronal cell damage, we treated LPS (0.2 μg/mL) to BV-2 cells with INF-γ (Thermo Scientific, 100 U/mL) after pre-treatment with the CMST and incubated for 24 hours under the condition of 37°C in 5% CO_2 in the cell incubator.

2.5. Immunostaining

Mice were anesthetized with intraperitoneal sodium pentobarbital (50 mg/kg) and trans-cardinally perfused with heparinized phosphate-buffered saline (PBS, pH 7.4), followed by perfusion with 4% paraformaldehyde in PBS. The brains were removed, immersed in the same fixative overnight, and cryoprotected in a 10%, 20%, and 30% sucrose solution. The brains were embedded in tissue freezing medium and frozen rapidly in 2-methyl butane precooled to its freezing point with liquid nitrogen.

The primary antibodies used for IF analysis, free-floating sections prepared one and applied to as follows; anti-rabbit cleaved caspase-3 antibody (CST, #9664) , anti-rabbit 53bp1 antibody (Abcam, Cabbridge, UK, ab36823), and anti-rabbit γH2AX antibody (CST, #7631), respectively. After overnight of primary for overnight and washing then applied secondary were incubated with secondary antibody which was goat-anti rabbit Alexa 488 fluorescence conjugated antibody then the nucleus was detected by hochest staining. For immunocytochemistry for cells, we followed to standard protocol for detecting fluorescence signals including anti-rabbit HIF-1α antibody (CST, #3716, 1:100) with anti-mouse cytochrome *c* antibody (Thermo Fischers, # 33-8500, 1:100), anti-rabbit cleaved caspase-3 antibody, anti-mouse 4-HNE antibody (Abcam, #ab48506, 1:100), and anti-mouse SOD2 antibody (Santa Cruz Biotechnology, #sc-133134, 1:100), respectively. The signals of fluorescence were detected using goat-anti mouse Alexa 594 fluorescence conjugated

Preprints (www.preprints.org) | NOT PEER-REVIEWED | Posted: 10 November 2019

antibody (Thermo Fischers, # A32742, 1:200) and donkey-anti rabbit Alexa 488 fluorescence conjugated antibody (Thermo Fischers, # A32790, 1:200). Nuclear staining was performed with Hoechst 33342 (H3570; Invitrogen). For quench the signals of oxidative stressor, DHE (D1168; Invitrogen) and Cell ROX Green Reagent (C10444; Thermo Fisher Scientific) were applied as well. All immunoreactions were observed under Axiophot microscope (Carl Zeiss) and confocal laser scanning microscope.

2.6. Immunoblot analysis

Tissue protein and cell lysates were collected by scraping, and the pellet was solubilized in lysis buffer (1×RIPA buffer, No. 9806; Cell Signaling). After centrifugation, protein concentrations were determined in supernatants using MicroBCA protein assay kits. Aliquots containing 30 µg protein were resolved by 10% sodium dodecyl sulfate/polyacrylamide gel electrophoresis. The blot was incubated with the primary antibodies: anti-p-Tau (1:1000, SC-101817; Santa Cruz Biotechnology), anti-p-p65 (1:1000, No. 3033S; Cell Signaling), anti-p65 antibody (1:1000, CST), anti-IκBα (1:1000, No. MA5-15132; Thermo Fisher Scientific), anti-HO-1 (1:1000, SC-10789; Santa Cruz Biotechnology), respectively. Membranes were washed and incubated for 2 h with a peroxidase-labeled secondary antibody. After three more washes, immunolabeled proteins were detected by chemiluminescence using a SuperSignal enhanced chemiluminescence (ECL) kit

2.7. Biochemical analysis

Preprints (www.preprints.org) | NOT PEER-REVIEWED | Posted: 10 November 2019

Total GSH content was determined by the previous method [19], and briefly, 50 µL of brain tissue homogenate which were diluted in 10 mM PBS (pH 7.2) or GSH standard was mixed with a total 80 µL of DTNB/NADPH mixture (10 µL 4 m DTNB with 70 µL 0.3 mM NADPH) into a 96-well microplate. Then, transferred 20 µL (0.06 U) of GSH-Rd to the same wells and final detectable products were determined under the condition of 412 nm absorbance using a spectrophotometer (Molecular Devices).

Total antioxidant capacity (TAC) in the brain tissue was assessed according to previous method which was published elsewhere the using myoglobin solution with 2,2'-azino-bis (3-ethylbenzothiazoline-6-sulfonic acid) diammonium salt (ABTS) [20]. The mixtures of myoglobin/ABTS solution and samples were reacted for 2 min at 25 °C, then 2.5 mM H_2O_2 was added as stop solution for 5 min and measured absorbance at 600 nm using a spectrophotometer. TAC was expressed as Trolox acid equivalent antioxidant capacity.

SOD activity was analyzed using a SOD assay kit (Millipore-Sigma), according to the manufacturer's protocol. Briefly, 20 µL of homogenate was mixed with 200 µL of WST-1 working solution in a 96-well plate. Then, 20 µL of working enzyme solution was added, and the plate was incubated for 20 min at 37C. Absorbance was measured at 450 nm using a UV spectrophotometer (Molecular Devices). A serial dilution of bovine erythrocyte SOD (Sigma) ranging from 0.01 to 50 U/mL was used as the standard.

Catalase activity was assayed as previously described [21]. Briefly, 30 µL of phosphatase buffer (250 mM, pH 7.2), 50 µL of 12 mM methanol, and 10 µL of 44 mM H_2O_2 were mixed with 60 µL of each homogenate sample or standard solution in a 96-well microplate. The reactions were allowed to proceed for 10 to 20 min and were stopped with the addition of 90 µL of Purpald

Preprints (www.preprints.org) | NOT PEER-REVIEWED | Posted: 10 November 2019

solution (22.8 mM Purpald in 2 N potassium hydroxide). The mixture was kept at 25 °C for 20 min, followed by the addition of 30 µL of potassium periodate (65.2 mM potassium periodate in 0.5 N potassium hydrate). The absorbance of the purple formaldehyde adduct that formed was measured at 550 nm using a spectrophotometer (Molecular Devices).

For measuring of caspase-3 and 7 activities, protein and cellular lysates were acquired followed by manufacture' protocol (CaspACE™ Assay System, Colorimetric, Promega).

2.8. Determination of cytokine levels

Protein levels of TNF-a, IL-6, IL-1b, and IL-10 in brain tissue were measured using commercial enzyme-linked immunosorbent assay kits (BioSource, San Jose, CA; R&D Systems), following the manufacturer's protocols.

2.9. Gene expression analysis by quantitative real-time PCR

Expression of the genes encoding for endogenous antioxidant related gene was measured by quantitative real-time PCR. Total RNA was isolated from brain tissue in RNAlater using an RNeasy Midi Kit (QIAGEN, CA, USA). The cDNA was synthesized by using a High-Capacity cDNA reverse transcription kit (Ambion, Austin, TX, USA). The real-time PCR was performed by using SYBR Green PCR Master Mix (Applied Biosystems, Foster City, CA, USA), and PCR amplification was performed using a standard protocol with the IQ5 PCR Thermal Cycler (Bio-Rad, Hercules, CA, USA). GAPDH was use as housekeeping gene and sequences for the used in the present study were summarized in Table 1.

2.10. Statistical analysis

Preprints (www.preprints.org) | NOT PEER-REVIEWED | Posted: 10 November 2019

All data are expressed as the mean ± standard error mean (SEM). Statistically significant differences between the groups were analyzed by one-way analysis of variance (ANOVA) followed by post hoc multiple comparison Fisher's LSD t-test using the IBM SPSS statistics 20.0 (SPSS Inc. Chicago, IL, USA). Differences at $p < 0.05$, $p < 0.01$, or $p < 0.001$ were considered statistically significant.

Preprints (www.preprints.org) | NOT PEER-REVIEWED | Posted: 10 November 2019

Results

3.1. Chemical composition analysis of CMST

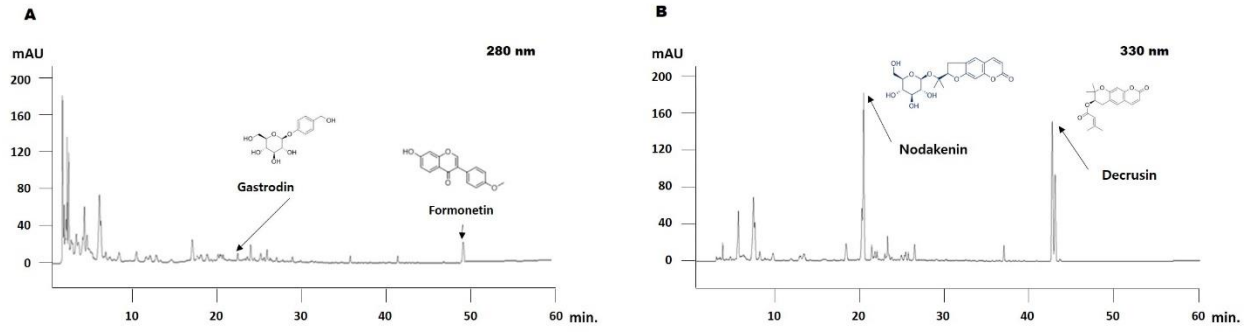

C **Chemical compositions of CMST**

Plant name	Chemicals	Wavelength (nm)	Retention time (min)	Concentration (ug/mL)
G.elata Blume	Gsatrodin	280	22.8	0.59 ± 0.004
A. mongholicus Bunge	Formonetin	280	48.7	1.83 ± 0.021
A. gigas Nakai	Nodakenin	330	20.8	91.19 ± 0.164
	Decursin	330	43.4	79.02 ± 0.141

Figure 1. Histogram of Chemical Composition analysis of CMST. Fingerprinting analysis was performed by high-performance liquid chromatography - diode array detector for detecting chemical composition analysis of CMST. Histogram major compounds from the CMST were detected by 280 nm (A) and 330 nm (B). The retention time and qualifications of each compounds were calculated (C).

Chemical compositional analyses for reference chemicals compounds from CMST were performed using HPLC-DAD. The histogram of CMST detected that four different chemical compounds, including gsatrodin, formonetin, nodakenin, and decrusin under the wavelength of 280- and 330-nm respectively (gsatrodin from *G.elata* Blume and formonetin from *A. mongholicus* Bunge were detected at 280 nm; nodakenin and decrusin were from *A. gigas* Nakai were detected at 330 nm, respectively). The retention time of gasdtrodin was for 22.8 min, and formonetin was for 48.7 min under the 280 nm of detection condition. Under the 330 nm of wavelength condition,

Preprints (www.preprints.org) | NOT PEER-REVIEWED | Posted: 10 November 2019

two of compounds such as nodakenin and decrusin from *A. gigas* Nakai were observed at the retention time of 20.8- and 43.4-min, respectively (Fig. 1-A and B). The quantification analysis data showed that gasdtrodin for 0.59 ± 0.004 μg/mL, formonetin for 1.83 ± 0.021 μg/mL, nodakenin for 91.19 ± 0.164 μg/mL, and decrusin for 79.02 ± 0.141 μg/mL, respectively (Fig. 1-C).

3.2. CMST Attenuates Hippocampus Neuronal Damages by Oxidation

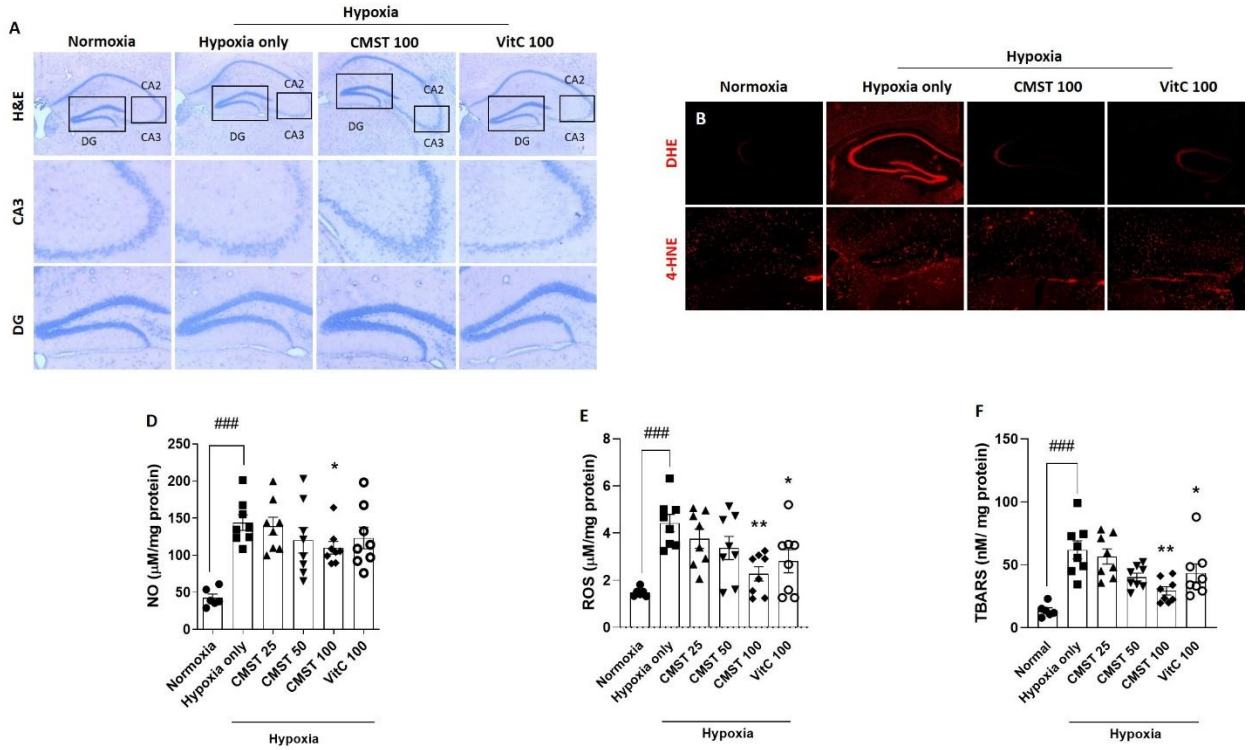

Figure 2. Pathological alterations of brain tissue and effects of the CMST on the oxidative stress during hypoxia. Histopathological analysis of brain tissue damage was captured by H&E staining (A) and detection of superoxide radicals by quenching of DHE staining (E), immunofluorescence analysis against 4-HNE (C), respectively. Hippocampal neuronal protein levels of NO (D), ROS (E), and TBARS (F) were also measured. Data were expressed mean ± S.E.M. (n = 6 to 8). $^{###}p< 0.001$ for Normoxia vs. Hypoxia only; $^{*}p < 0.05$ and $^{**}p < 0.01$ for Hypoxia only vs. CMST or Vit C 100. The images for H&E stains were captured under the light microscopy environment (40 × or 100 × magnification) and fluorescence signals were captured by fluorescence filters equipped microscopy condition (40 × magnification).

Preprints (www.preprints.org) | NOT PEER-REVIEWED | Posted: 10 November 2019

We examined histopathological analysis whether CMST improved the hypoxic condition-induced brain injury or not. Our H&E staining results displayed that hippocampus area, especially CA2 and CA3 zones, and dentate gyrus (DG) area were severely altered by hypoxia. Administration with CMST, however, the above tissue injuries were notably recovered (Fig. 2-A). In addition, CMST exerted to diminish the above pathological alterations of brain tissue injuries due to excessive oxidative stress droning hypoxic condition which were evidenced by acceleration of DHE signals and IF analysis against 4-HNE in the brain tissue (especially 100 mg/kg of treatment group, Fig. 2-B and C, part of red fluorescence). Biochemical analysis of oxidative stress parameters, such as ROS and NO were drastically increased by 2.9- and 3.4-fold, and final product of oxidative stress, lipid peroxidation levels which was measured by TBARS in the present study were approximately 4.5-fold altered in an increase mode as compared with normoxia group; whereas administration with CMST significantly decreased the pathological alterations (Fig. 2-D and F, $p < 0.05$ for NO, $p < 0.01$ for ROS and TBARS, respectively).

Administration with Vit C (100 mg/kg) showed similar properties of CMST (100 mg/kg) in histopathological analysis of H&E staining, DHE assay and IF against 4-HNE. The protein levels of ROS and TBARS were significantly attenuated by Vit C, but not NO levels ($p < 0.05$ vs. Hypoxia only).

3.3. CMST Prevented from Deterioration of Atioxidant components in Neuronal Cell Injury

Severe depletion of endogenous antioxidant components in hippocampal neuronal cells were observed in hypoxia group; deteriorations of the total GSH contents, TAC, SOD activities, and catalase activities were decreased approximately 0.34-, 0.36-, 0.31-, and 0.29-fold as compared

Preprints (www.preprints.org) | NOT PEER-REVIEWED | Posted: 10 November 2019

with normoxia group. Administration with CMST, especially 100 mg/kg, however significantly reduced and prevented from oxidative stress and antioxidant depletion from hypoxia condition (Fig. 3-A to D, $p < 0.05$ for SOD activities and catalase activities, $p < 0.01$ for TAC, respectively).

The antioxidant components were significantly blocked the deteriorations of antioxidant components which were similar effects as CMST ($p < 0.05$ vs. Hypoxia only).

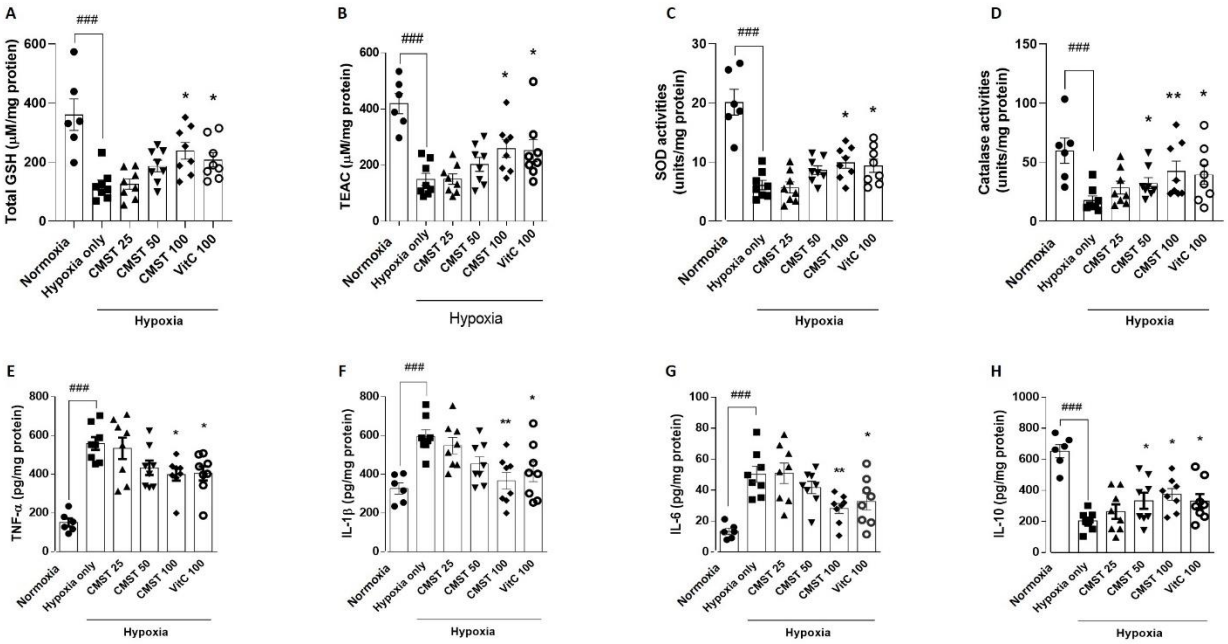

Figure 3. Effects of the CMST on the Endogenous antioxidants and inflammatory cytokines in the hippocampaus neuronal cells. Protein levels of endogenous antioxidants including total GSH (A), TEAC (2), SOD activities (C), and catalase activities (D) were measured. Pro-inflammatory cytokines including TNF-α (E), IL-1β (F), IL-6 (G), and anti-inflammatory cytokine such as IL-10 (H) were analyzed in the hippocampus. Data were expressed mean ± S.E.M. (n = 6 to 8). ###p< 0.001 for Normoxia vs. Hypoxia only; * p< 0.05 and **p < 0.01 for Hypoxia only vs. CMST or Vit C 100.

3.4. CMST Improved Inflammatory Reactions during Hypoxic Condition

Pro-inflammatory cytokines inducing TNF-α, IL-1β, and IL-6 were drastically increased around 3.7-, 1.8-, and 3.8-fold as compared with normoxia group, whereas administration with

Preprints (www.preprints.org) | NOT PEER-REVIEWED | Posted: 10 November 2019

CMST significantly led to reduce the abnormal elevations of pro-inflammatory cytokines (Especially CMST 100 group; Fig. 3-E to G, $p < 0.05$ for TNF-α and $p < 0.01$ for IL-1β and IL-6, respectively). The anti-inflammatory cytokine, IL-10, was decreased by hypoxia as 0.3-fold comparing to normoxia group; however, administration with 100 mg/kg of CMST improved the alterations with statistical significance (Fig. 3-H, $p < 0.05$).

Administration with VitC 100 also showed beneficial effects on the inflammatory reactions similarly to CMST as compared with hypxia group (Fig. 3-E to H, $p < 0.05$).

3.5. Effects of CMST on the Hippocampus Neuronal Cell Death

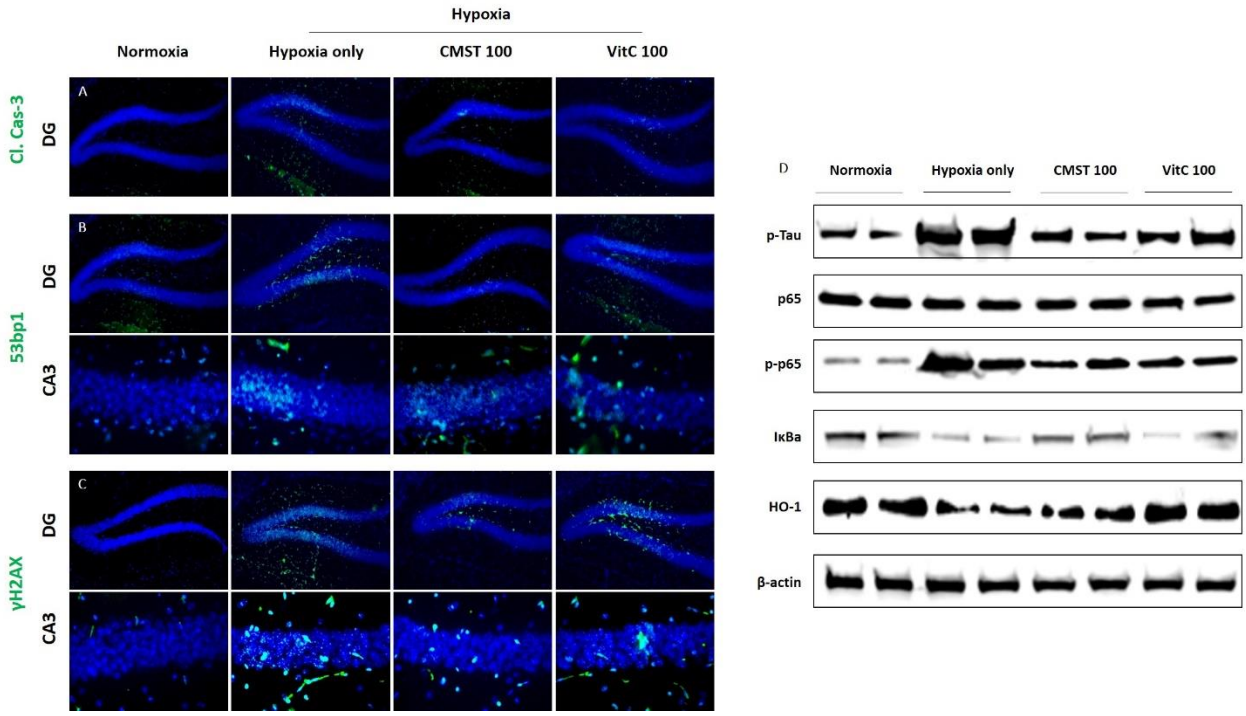

Figure 4. Representative IF analysis of DNA fragment and programmed cell death related molecules, and Western blot analysis for brain neurodegenerations and inflammation. Representative immunofluorescence analysis against cleaved caspase-3 (A), 53bp1 (B), and γH2AX (C) in the hippocampus neuronal cells areas. Western blot analysis for p-Tau, p-p65, p65, IκBα, HO-1, and β-actin was used as inner control (D). The images for fluorescence signals were captured by fluorescence filters equipped microscopy condition (100 × for dentate gyrus and 400 × for CA3 zone, respectively).

Preprints (www.preprints.org) | NOT PEER-REVIEWED | Posted: 10 November 2019

We next addressed to cell death related molecules which is cleaved form of caspase-3, especially programmed cell death called apoptosis in the hypoxia model. As our expectation, the DG regions of hippocampus area were enhanced positive signals of cleaved form of caspase-3, and DNA fragmentation markers such as 53bp1 and γH2AX signals in the nucleic area in the DG and CA3 zones of hypxia only group were drastically increased as compared with normoxia group (Fig. 4-A to C, Part of green fluorescence). The above abnormal alterations were notably reduced by CMST administrations (Fig. 4-A to D).

Western blot analysis for neuronal cell injury molecule, p-Tau, were considerably increased in hypoxia group, and key molecules for oxidation and inflammatory reactions such as NF-κB and IκBα were also abnormally altered according our expectation. Additionally, an enzyme which can regulate antioxidant status by various stress reactions in the brain tissue, called HO-1 was drastically depleted in hypoxia only group as compared with normoxia group. The above alterations were notably improved by administration with CMST (Fig. 4-E).

VitC 100 also showed beneficial effects on the hypoxic condition as similar with CMST (Fig. 4-A to E).

3.6. CMST Attenuated Hippocampus Neuronal Cell Death via Regulation of Oxidative Stress

Our cell based *in vitro* experiment using mouse derived hippocampus neuronal cell line, HT-22 cells, were well represented hypoxia condition by enhancement of HIF-1α (part of green fluorescence) and apoptotic cell death markers of cytochrome *c* positive cells (part of red fluorescence, Fig. 5-A). These results are well matched with higher signals of pro-apoptosis

Preprints (www.preprints.org) | NOT PEER-REVIEWED | Posted: 10 November 2019

molecules, cleaved-caspase 3, and increases of 4-HNE positive cells (Fig. 5-B and C). Whereas, SOD-2 positive signals were decreased in hypoxia condition as compared with normoxia group (Fig. 5-D). Cellular levels of caspase-3/7, ROS, TBARS were abnormally elevated, while total GSH contents, SOD activities, and catalase activities were decreased by hypoxia as compared with normoxia (Fig. 5-E to J, $p < 0.05$ or 0.01 for CMST 50 or 100 μg/mL). Gene expression levels of antioxidant components including Gss, Grd, Sod1, Sod2, Sod3, and Cat were lowered as 0.27-, 0.26-, 0.31-, 0.26, and 0.24-fold lowered than that of normoxia group, and these alterations were significantly normalized (Fig. 5-K, $p < 0.05$ or 0.01 for CMST 50 or 100 μg/mL).

Vitamin C (100 μg/mL) also showed similar effects on the HT-22 cells which were induced by hypoxia ($p < 0.01$or $p < 0.001$, Fig. 5-A to J).

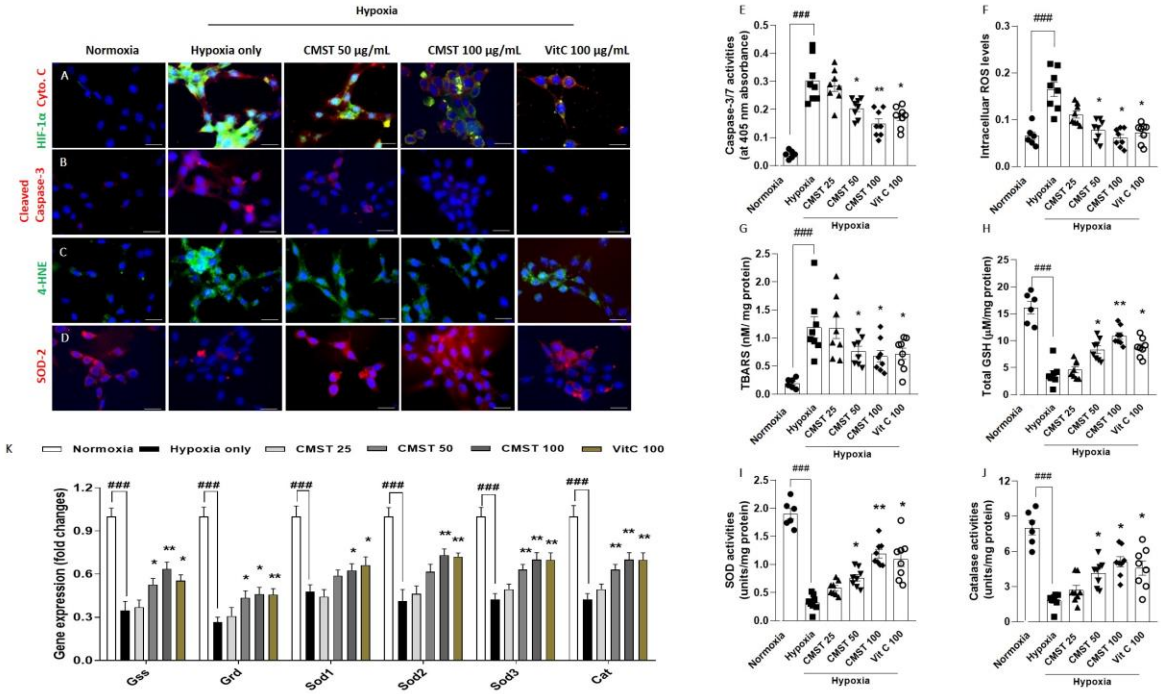

Figure 5. ***In vitro*** **analysis of hippocampal neuronal cell damage using mouse derived hippocampal cell line, HT-22 cells under the hypoxic-condition.** Representative immunofluorescence images for HIF-1α and cytochrome *c* (green fluorescence for HIF-1α and red fluorescence for cytochrome *c* (A), cleaved

Preprints (www.preprints.org) | NOT PEER-REVIEWED | Posted: 10 November 2019

caspase-3 (B), 4-HNE (C), and SOD-2 (D). Cellular protein levels of caspase-3/7 activities (E), intracellular ROS (F), TBARS (G), total GSH contents (H), SOD activities (I), and catalase activities (J). Gene expression analysis was performed using qPCR and GAPDH was used as a house keeping gene (K). The immunostainings were captured by fluorescence filters equipped microscopy condition (630 × magnification). Data were expressed mean ± S.E.M. (n = 6 to 8). $^{###}p< 0.001$ for Normoxia vs. Hypoxia only; $^{*}p < 0.05$ and $^{**}p < 0.01$ for Hypoxia only vs. CMST or Vit C 100.

3.7. CMST Attenuated Hippocampus Neuronal Cell Death via Regulation of Oxidative Stress

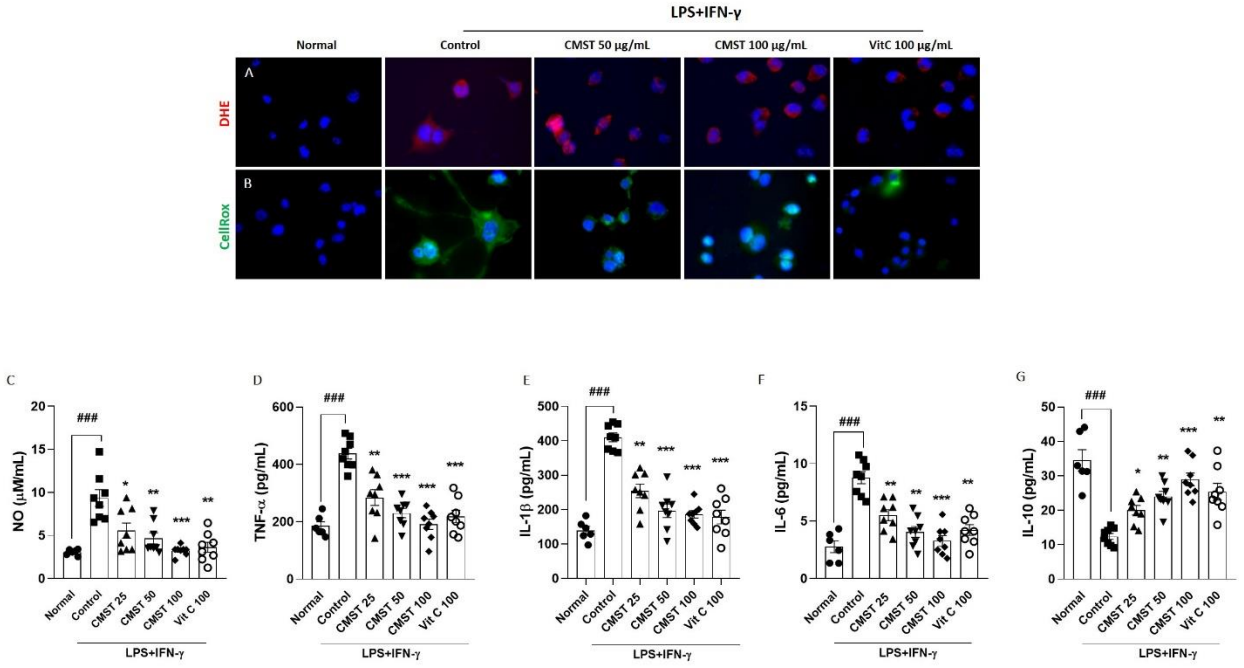

Figure 6. *In vitro* analysis of microglial cells activation using mouse derived hippocampal cell line, BV-2 cells. Mouse derived microglia cells, BV-2 cells, were artificially activated by lipopolysaccharide (LPS, 0.2 μg/mL) with interferon-γ (100 units/mL) for 18 hours with/without condition of CMST in a various dose 4 hours before treatment. The images for fluorescence signals were captured by fluorescence filters equipped microscopy condition (630 × magnification). Representative immunofluorescence analysis for detection of DHE (A) and CellRox (B). Cellular levels of NO (C), TNF-α (D), IL-1β (E), IL-6 (F), and IL-10 were analyzed. Data were expressed mean ± S.E.M. (n = 6 to 8). $^{###}p< 0.001$ for Normal *vs.* Control; $^{*}p< 0.05$ and $^{**}p < 0.01$ for Control *vs.* CMST or Vit C 100.

Preprints (www.preprints.org) | NOT PEER-REVIEWED | Posted: 10 November 2019

To assess the underlying actions of CMST on the neuronal cell death during hypoxic condition, especially microglial activations-mediated condition, we induced microglial activations by LPS treatment with IFN-γ stimulations. We detected ROS signals using DHE and Cell ROX in the above condition, and CMST drastically reduced these abnormal elevation of ROS signals (Fig. 6 - A and B). In addition, the level of NO from the supernatant was also decreased by CMST (Fig. 6-C). Pre-treatment with CMST also significantly reduced pro- or anti-inflammatory cytokines including IL-1β, IL-6, and IL-10 as compared with control group (Fig. 6-D to G, $p < 0.05$, $p < 0.01$, and $p < 0.05$ in the CMST treated group as compared with control group).

The above alterations were also well normalized by pre-treatment with VitC 100 μg/mL with statistical significance ($p < 0.01$ or $p < 0.001$, Fig. 6-A to G).

Preprints (www.preprints.org) | NOT PEER-REVIEWED | Posted: 10 November 2019

Discussion

We purposed to demonstrate pharmacological properties and underlying actions of a new prescribed-medicinal herbal remedy, called CMST, against a severe neurodegenerative disease condition. Among the various preclinical animal models of neurogenerative diseases, we selected hypoxia-induced brain injury model, which can accelerate neuronal cell injury with enhancement of cell death signaling via excessive generations of oxidative stress [22-24] than other animal models. Herein we also observed neuronal cell injury in the brain tissue with severe enhancement of oxidative stress, by performance of H&E staining and DHE, and IHC analysis against 4-HNE, especially hippocampus areas, respectively (Fig. 2- A to E).

Emerging evidences mentioned that excessive generations of free radicals (i.e, ROS and NO) lead to accelerations brain tissue injuries [25-27]. Above pathological conditions were well correlated with depletion of non-enzymatic antioxidant components as well as enzymatic-antioxidant in the hippocampus area of brain tissue (Fig. 3-A to D). Administrations with CMST not only notably reduced oxidative stress, but also efficiently prevented from depletions of antioxidant components comparing to hypoxia only group (especially in 100 mg/kg, $p < 0.05$ or 0.01). Damages from oxidative stress is deeply associated with inflammations and coordinates for stimulating of cell death signaling pathways. We supplemented that CMST significantly normalized against abnormal status of pro- and anti-inflammatory cytokines (especially in 100 mg/kg, $p < 0.05$ or 0.01, Fig. 3-E to H).

Eventually, accumulation of oxidative stress promotes cellular damages via enhancing of cell death related molecules by oxidative stress provoked DNA fragmentations [28, 29]. Programmed cell death was generated during hypoxia [25, 30, 31], and CMST drastically exerted to reduce

Preprints (www.preprints.org) | NOT PEER-REVIEWED | Posted: 10 November 2019

cleaved caspase-3 in the hippocampus area, especially DG zones (Fig. 4-A). Moreover, this pharmacological property was also well adapted to decreases positive signals of DNA fragmentation which were evidenced by enhancement of 53bp1 and γH2AX, respectively (Fig. 4-B and C). In the present study, the pharmacological effects of CMST also reached out normalization of p-Tau in the hippocampus protein, and it normalized pivotal factors of inflammatory reactions, such as p-NFκB and IκBα as well. Additionally, another critical enzyme against various types of stress responses was also improved by CMST (Fig. 4-D).

Under the hypoxic-condition, oxidation and inflammation coordinate cell death as well as microglial activations [32, 33]. We further examined that CMST ameliorated hypoxia mediated neuronal cell death and oxidations by IF analysis (Fig. 5-A to D), and these properties were well supported cellular protein and gene expression levels in prompt manners ($p < 0.05$ or 0.01 for 50 or 100 μg/mL Fig. 5-E to K). Regarding microglial activations by hypoxia [32-34], CMST considerably attenuates generations of ROS as well as inflammatory cytokines (Fig. 6-A to G, $p < 0.05$ or 0.01,). Consistent with anti-inflammatory effects, pre-treatment with the CMST also atteunated oxidative stress signaling by detection of NO levels in media, and DHE and CellRox signaling (Fig. 6-A to C, $p < 0.05$, $p < 0.01$, and $p < 0.05$ in the CMST treated group as compared with control group for NO levels).

Unfortunately, there is no effective therapeutics for treating neurodegeneration in recent days and pathophysiological mechanisms remains still unclear. Therefore, many of study groups have tried to reveal the exact mechanism and develop drug remedy worldwide. In the present study, we also considered the above critical issue and finally prescribed new combinations of medicinal herbs, CMST, which is purposed to treat the patients with neurodegenerative diseases in clinical practice of TKM area. We provided the pharmacological effects of CMST on the hippocampus neuronal

Preprints (www.preprints.org) | NOT PEER-REVIEWED | Posted: 10 November 2019

cell damages by prevent from cell death signaling as well as inhibition of microglial activations. The pharmacological actions of CMST would be explained their major compounds; gsatrodin (from *G. elata* Blume,) is known for elimination of free radicals in a cognitive dysfunction by oxidative stress of ischemia rats [35], and it protected apoptotic dopaminergic neurons [36]. Formotenin affected to the various brain improved memory functions and endogenous redox status [14, 37, 38]. Evidenced by previous studies documented that decrusin and nodakein showed protective effects on primary cultured rat cortical cells from glutamate-induced neurotoxicity [39] and cognitive functional abilities [40].

Collectively, we convince that CMST shows its main pharmacological properties by modulations of endogenous redox system in neuronal cells, it also blocked inflammatory response due to microglial activation. The above actions then efficiently block neuronal cell death during hypoxia. Taken together, CMST would be applying to the various neurodegenerative diseases and further study will need to reveal its efficacies in the clinical trial applications.

Preprints (www.preprints.org) | NOT PEER-REVIEWED | Posted: 10 November 2019

Conflicts of interests

This study was financially supported by the National Research Foundation of Korea (NRF) grant No. 2019R1F1A1061062 and Ministry of Health & Welfare (H15C-0006-020019) for the Korean Medicine R&D Project from South Korea.

Preprints (www.preprints.org) | NOT PEER-REVIEWED | Posted: 10 November 2019

Acknowledgements

This study was financially supported by the National Research Foundation of Korea (NRF) grant No. 2019R1F1A1061062 and Ministry of Health & Welfare (H15C-0006-020019) for the Korean Medicine R&D Project from South Korea. HI15C0006-2019.

Preprints (www.preprints.org) | NOT PEER-REVIEWED | Posted: 10 November 2019

References

1. Casini, G.; Fontanesi, G.; Bingman, V. P.; Jones, T. J.; Gagliardo, A.; Ioale, P.; Bagnoli, P., The neuroethology of cognitive maps: contributions from research on the hippocampus and homing pigeon navigation. *Arch Ital Biol* **1997,** 135, (1), 73-92.
2. Chrousos, G. P.; Gold, P. W., The concepts of stress and stress system disorders. Overview of physical and behavioral homeostasis. *JAMA* **1992,** 267, (9), 1244-52.
3. Grady, C. L., Functional brain imaging and age-related changes in cognition. *Biol Psychol* **2000,** 54, (1-3), 259-81.
4. LeDoux, J. E., Emotion: clues from the brain. *Annu Rev Psychol* **1995,** 46, 209-35.
5. van Praag, H.; Fleshner, M.; Schwartz, M. W.; Mattson, M. P., Exercise, energy intake, glucose homeostasis, and the brain. *J Neurosci* **2014,** 34, (46), 15139-49.
6. Zachariae, R., Psychoneuroimmunology: a bio-psycho-social approach to health and disease. *Scand J Psychol* **2009,** 50, (6), 645-51.
7. Adonaylo, V. N.; Oteiza, P. I., Lead intoxication: antioxidant defenses and oxidative damage in rat brain. *Toxicology* **1999,** 135, (2-3), 77-85.
8. Carson, M. J.; Sutcliffe, J. G., Balancing function vs. self defense: the CNS as an active regulator of immune responses. *J Neurosci Res* **1999,** 55, (1), 1-8.
9. Buzanska, L.; Machaj, E. K.; Zablocka, B.; Pojda, Z.; Domanska-Janik, K., Human cord blood-derived cells attain neuronal and glial features in vitro. *J Cell Sci* **2002,** 115, (Pt 10), 2131-8.
10. Farina, C.; Aloisi, F.; Meinl, E., Astrocytes are active players in cerebral innate immunity. *Trends Immunol* **2007,** 28, (3), 138-45.

Preprints (www.preprints.org) | NOT PEER-REVIEWED | Posted: 10 November 2019

11. Zhang, Y.; Chen, K.; Sloan, S. A.; Bennett, M. L.; Scholze, A. R.; O'Keeffe, S.; Phatnani, H. P.; Guarnieri, P.; Caneda, C.; Ruderisch, N.; Deng, S.; Liddelow, S. A.; Zhang, C.; Daneman, R.; Maniatis, T.; Barres, B. A.; Wu, J. Q., An RNA-sequencing transcriptome and splicing database of glia, neurons, and vascular cells of the cerebral cortex. *J Neurosci* **2014,** 34, (36), 11929-47.

12. Floyd, R. A., Antioxidants, oxidative stress, and degenerative neurological disorders. *Proc Soc Exp Biol Med* **1999,** 222, (3), 236-45.

13. Herbert, V.; Shaw, S.; Jayatilleke, E.; Stopler-Kasdan, T., Most free-radical injury is iron-related: it is promoted by iron, hemin, holoferritin and vitamin C, and inhibited by desferoxamine and apoferritin. *Stem Cells* **1994,** 12, (3), 289-303.

14. Kim, H. G.; Lee, J. S.; Han, J. M.; Lee, J. S.; Choi, M. K.; Son, S. W.; Kim, Y. K.; Son, C. G., Myelophil attenuates brain oxidative damage by modulating the hypothalamus-pituitary-adrenal (HPA) axis in a chronic cold-stress mouse model. *J Ethnopharmacol* **2013,** 148, (2), 505-14.

15. Dringen, R., Oxidative and antioxidative potential of brain microglial cells. *Antioxid Redox Signal* **2005,** 7, (9-10), 1223-33.

16. Vilhardt, F., Microglia: phagocyte and glia cell. *Int J Biochem Cell Biol* **2005,** 37, (1), 17-21.

17. Gao, H. M.; Hong, J. S., Why neurodegenerative diseases are progressive: uncontrolled inflammation drives disease progression. *Trends Immunol* **2008,** 29, (8), 357-65.

18. Erkkinen, M. G.; Kim, M. O.; Geschwind, M. D., Clinical Neurology and Epidemiology of the Major Neurodegenerative Diseases. *Cold Spring Harb Perspect Biol* **2018,** 10, (4).

19. Ellman, G. L., Tissue sulfhydryl groups. *Arch Biochem Biophys* **1959,** 82, (1), 70-7.

Preprints (www.preprints.org) | NOT PEER-REVIEWED | Posted: 10 November 2019

20. Kambayashi, Y.; Binh, N. T.; H, W. A.; Hibino, Y.; Hitomi, Y.; Nakamura, H.; Ogino, K., Efficient assay for total antioxidant capacity in human plasma using a 96-well microplate. *J Clin Biochem Nutr* **2009,** 44, (1), 46-51.

21. Wheeler, C. R.; Salzman, J. A.; Elsayed, N. M.; Omaye, S. T.; Korte, D. W., Jr., Automated assays for superoxide dismutase, catalase, glutathione peroxidase, and glutathione reductase activity. *Anal Biochem* **1990,** 184, (2), 193-9.

22. Manukhina, E. B.; Goryacheva, A. V.; Barskov, I. V.; Viktorov, I. V.; Guseva, A. A.; Pshennikova, M. G.; Khomenko, I. P.; Mashina, S. Y.; Pokidyshev, D. A.; Malyshev, I. Y., Prevention of neurodegenerative damage to the brain in rats in experimental Alzheimer's disease by adaptation to hypoxia. *Neurosci Behav Physiol* **2010,** 40, (7), 737-43.

23. Nalivaeva, N. N.; Turner, A. J.; Zhuravin, I. A., Role of Prenatal Hypoxia in Brain Development, Cognitive Functions, and Neurodegeneration. *Front Neurosci* **2018,** 12, 825.

24. Snyder, B.; Shell, B.; Cunningham, J. T.; Cunningham, R. L., Chronic intermittent hypoxia induces oxidative stress and inflammation in brain regions associated with early-stage neurodegeneration. *Physiol Rep* **2017,** 5, (9).

25. Coimbra-Costa, D.; Alva, N.; Duran, M.; Carbonell, T.; Rama, R., Oxidative stress and apoptosis after acute respiratory hypoxia and reoxygenation in rat brain. *Redox Biol* **2017,** 12, 216-225.

26. Lewen, A.; Matz, P.; Chan, P. H., Free radical pathways in CNS injury. *J Neurotrauma* **2000,** 17, (10), 871-90.

27. Maiti, P.; Singh, S. B.; Sharma, A. K.; Muthuraju, S.; Banerjee, P. K.; Ilavazhagan, G., Hypobaric hypoxia induces oxidative stress in rat brain. *Neurochem Int* **2006,** 49, (8), 709-16.

Preprints (www.preprints.org) | NOT PEER-REVIEWED | Posted: 10 November 2019

28. Fricker, M.; Tolkovsky, A. M.; Borutaite, V.; Coleman, M.; Brown, G. C., Neuronal Cell Death. *Physiol Rev* **2018,** 98, (2), 813-880.

29. Kashiwagi, H.; Shiraishi, K.; Sakaguchi, K.; Nakahama, T.; Kodama, S., Repair kinetics of DNA double-strand breaks and incidence of apoptosis in mouse neural stem/progenitor cells and their differentiated neurons exposed to ionizing radiation. *J Radiat Res* **2018,** 59, (3), 261-271.

30. Liu, C. L.; Siesjo, B. K.; Hu, B. R., Pathogenesis of hippocampal neuronal death after hypoxia-ischemia changes during brain development. *Neuroscience* **2004,** 127, (1), 113-23.

31. Thornton, C.; Leaw, B.; Mallard, C.; Nair, S.; Jinnai, M.; Hagberg, H., Cell Death in the Developing Brain after Hypoxia-Ischemia. *Front Cell Neurosci* **2017,** 11, 248.

32. Cikla, U.; Chanana, V.; Kintner, D. B.; Covert, L.; Dewall, T.; Waldman, A.; Rowley, P.; Cengiz, P.; Ferrazzano, P., Suppression of microglia activation after hypoxia-ischemia results in age-dependent improvements in neurologic injury. *J Neuroimmunol* **2016,** 291, 18-27.

33. Kiernan, E. A.; Smith, S. M.; Mitchell, G. S.; Watters, J. J., Mechanisms of microglial activation in models of inflammation and hypoxia: Implications for chronic intermittent hypoxia. *J Physiol* **2016,** 594, (6), 1563-77.

34. Zhang, F.; Zhong, R.; Li, S.; Fu, Z.; Cheng, C.; Cai, H.; Le, W., Acute Hypoxia Induced an Imbalanced M1/M2 Activation of Microglia through NF-kappaB Signaling in Alzheimer's Disease Mice and Wild-Type Littermates. *Front Aging Neurosci* **2017,** 9, 282.

Preprints (www.preprints.org) | NOT PEER-REVIEWED | Posted: 10 November 2019

35. Li, Y.; Zhang, Z., Gastrodin improves cognitive dysfunction and decreases oxidative stress in vascular dementia rats induced by chronic ischemia. *Int J Clin Exp Pathol* **2015,** 8, (11), 14099-109.

36. Kumar, H.; Kim, I. S.; More, S. V.; Kim, B. W.; Bahk, Y. Y.; Choi, D. K., Gastrodin protects apoptotic dopaminergic neurons in a toxin-induced Parkinson's disease model. *Evid Based Complement Alternat Med* **2013,** 2013, 514095.

37. Kim, H. G.; Lee, J. S.; Choi, M. K.; Han, J. M.; Son, C. G., Ethanolic extract of Astragali radix and Salviae radix prohibits oxidative brain injury by psycho-emotional stress in whisker removal rat model. *PLoS One* **2014,** 9, (5), e98329.

38. Lee, J. S.; Kim, H. G.; Han, J. M.; Kim, D. W.; Yi, M. H.; Son, S. W.; Kim, Y. A.; Lee, J. S.; Choi, M. K.; Son, C. G., Ethanol extract of Astragali Radix and Salviae Miltiorrhizae Radix, Myelophil, exerts anti-amnesic effect in a mouse model of scopolamine-induced memory deficits. *J Ethnopharmacol* **2014,** 153, (3), 782-92.

39. Kang, S. Y.; Kim, Y. C., Decursinol and decursin protect primary cultured rat cortical cells from glutamate-induced neurotoxicity. *J Pharm Pharmacol* **2007,** 59, (6), 863-70.

40. Gao, Q.; Jeon, S. J.; Jung, H. A.; Lee, H. E.; Park, S. J.; Lee, Y.; Lee, Y.; Ko, S. Y.; Kim, B.; Choi, J. S.; Ryu, J. H., Nodakenin Enhances Cognitive Function and Adult Hippocampal Neurogenesis in Mice. *Neurochem Res* **2015,** 40, (7), 1438-47.

Preprints (www.preprints.org) | NOT PEER-REVIEWED | Posted: 10 November 2019

Table 1. Sequence of the primers used in real-time PCR analysis

Gene list	Primer sequencing (Forward and Reverse)	Product size (base pair)	Annealing temperature (°C)
Catalase	5'-CTG GGA TCT TGT GGG AAA CAA-3' 5'-GTG AGT CTG TGG GTT TCT CTT CTG-3'	100	58
Glutathione-synthase	5'-ACC GAA GGC TGT TTA TGG ATG A-3' 5'-AGG CGT GCT TCC CAG TTC T-3'	100	59
Glutathione-reductase	5'-CGA TGT ATC ACG CTG TGACC-3' 5'-GGT GAC CAG CTC CTC TGA AG-3'	120	58
SOD-1	5'-TGT CAG GAC AAA TTA CAG GAT TAA CTG-3' 5'-AAA TGA GGT CCT GCA CTG GTA CA-3'	100	60
SOD-2	5'-CCCAGACCTGCCTTACGACTAT-3' 5'-GGTGGCGTTGAGATTGTTCA-3'	112	58
SOD-3	5'-GGT GGA TGC TGC CGA GAT-3' 5'-GCT GCC GGA AGA GAA CCA A-3'	101	59
GAPDH	5'-TCA CTC AAG ATT GTC AGC AAT GC-3' 5'-GGC CCC GGC CTT CTC-3'	100	58